OPEN

Improved Cuff Technique and Intraoperative Detection of Vascular Complications for Hind Limb Transplantation in Mice

Minhyung Kim, MD,[1,2] Daniel T. Fisher, PhD,[1,2] Colin A. Powers, MD,[1,2] Elizabeth A. Repasky, PhD,[2] and Joseph J. Skitzki, MD[1,2]

Background. Vascularized composite tissue allotransplantation (VCA) from a cadaveric donor has now become a clinical reality and the treatment modality of choice for patients with devastating injuries, deformities, and complex tissue defects. However, many VCA patients experience severe toxicities due to the strong immunosuppression required secondary to high antigenicity of the grafts. To improve immunosuppressive protocols for VCA, feasible and reliable preclinical models are necessary. The purpose of this study was to introduce new techniques to an established preclinical VCA model to accelerate future investigations. **Methods.** C57BL/6 (H-2^b) and BALB/c (H-2^d) mice were used to perform VCA as recipients and donors, respectively. Surgery time, success rate, associated complications, and mortality were analyzed. Blood flow in grafts was interrogated with laser speckle image (LSI). **Results.** A nonsuture cuff technique was used with the abdominal aorta for end-to-end anastomosis. The cuff technique demonstrated efficiency for donor surgery (52 ± 10 minutes for donor vs. 45 ± 8 minutes for recipient surgery). Successful revascularization was achieved in 27 (90%) of 30 transplants. The majority of surgical complications occurred within 48 hours including artery occlusion, venous occlusion, cerebral stroke, and minor bleeding without mortality. LSI was useful in detecting intraoperative vascular complications with display patterns predictive of complication type. **Conclusions.** The described techniques may facilitate a more efficient heterotopic hind limb transplantation mouse model of VCA.

(Transplantation Direct 2018;4: e345; doi: 10.1097/TXD.0000000000000756. Published online 24 January, 2018.)

New microsurgical techniques and powerful immunosuppressive drugs have made it possible for severely injured patients to receive composite tissue allografts to

replace limbs, hands, and faces, vastly improving the quality of life.[1-4] However, although tremendous progress has been made in the 20 years since the first successful hand transplant,[5] there are significant challenges preventing its widespread acceptance and use. A major problem is the severe shortage of donors with a close HLA match. Also, the complexity of vascularized composite tissue allotransplantation (VCA) lies in the fact that there are multiple tissue types, most importantly, the skin, which is highly immunogenic and the primary target of T cell–mediated destruction of allografts.[6] Dendritic cells in the skin are the critical causes of this problem because they are known to migrate from donor skin to recipient lymph nodes where they activate donor- and recipient-specific CD4^{+} T cells capable of recognizing mismatched graft HLA molecules.[7-9] With the elaboration of the immune reaction, cytotoxic effector CD8^{+} T cells then migrate into the graft and initiate rejection of the VCA.[10,11] As a result, the rejection rates of composite grafts remain high and the associated toxicity of the strong immunosuppressive regimens required to maintain these allografts is problematic. Although, a VCA can provide a significant increase in quality of life, far too many of these patients experience the disappointment of either graft rejection or increased risk of additional health problems, such as renal toxicity and higher incidences of cancer from the lifelong use of high-dose immunosuppressive drugs.[12] To improve on the immunosuppressive protocols

TABLE 1.

Mouse haplotype

Mouse strain		MHC haplotype	MHC class I			MHC class II	
			H-2K	H-2D	H-2L	I-A	I-E
BALB/c	Donor	d	d	d	d	d	d
C57BL/6	Recipient	b	b	b	-	b	-

used to maintain a VCA, a feasible and reliable preclinical model could be impactful.

Advantages of a mouse model for VCA include the fact that the murine H-2 system is similar to the human HLA system and the mice are capable of allograft rejection. In addition, the number of gene knockout mouse models and the broad range of established mouse reagents may allow for a more thorough investigation of VCA rejection mechanisms and the development of immunosuppression protocols. Despite the fact that advanced microsurgical techniques facilitated the success of VCA, mouse models have proven to be technically demanding and physiologically fragile, resulting in limited use.[13,14] Technical difficulties are mainly due to the small diameters of murine vessels and the resulting surgical complications after vascular anastomosis using suture techniques. Although high success rates of graft revascularization with a nonsuture "cuff technique" are possible,[15] long donor surgery time and intraoperative vascular complications still remain as challenges.

As opposed to existing techniques, we developed a modified cuff method using the abdominal aorta (AA) rather than the femoral artery. For graft evaluation we employed a laser speckle image (LSI) system for detecting intraoperative vascular complications as an aid to facilitate successful microsurgical transplantation. Herein we described the method in detail and show the advantages of this new approach.

MATERIALS AND METHODS

Mice

Female C57BL/6 (H-2b) and BALB/c (H-2d) mice aged 7 to 8 weeks were purchased from Charles River (Kingston, NY) as recipients and donors respectively (Table 1). Mice were fed a standard laboratory diet and housed under standard light and accommodation conditions.

Periprocedural Care

A total of 30 heterotopic cervical hind limb transplantations were performed. All operations were carried out under sterile conditions, with animals kept on a heating plate at 37.5°C. Immediately before surgery, mice underwent anesthetic induction with 4% isoflurane inhalation (Abbott Laboratories, Chicago, IL). Anesthesia was maintained with 2% isoflurane inhalation via a nose cone. Puralube ophthalmic ointment (Dechra Veterinary Products, Overland Park, KS) was applied for eye protection. All recipient mice were recovered on a warming blanket, injected subcutaneously with buprenorphine (0.2 mg/kg body weight) for pain control every 8 hours, and given saline (1.0 mL) subcutaneously to prevent dehydration. All experimental protocols were approved by the Roswell Park Cancer Institutional Animal Care and Use Committee.

Donor Procedure

The abdomen and the left groin of the donor mouse was shaved, disinfected with alcohol, and draped for complete exposure. A laparotomy was made through an abdominoinguinal incision (midline abdomen with bilateral extensions over each groin). After displacing the small bowel and cecum to the right side of the abdominal cavity, the AA was identified with the use of a dissecting microscope (VWR, West Chester, PA), with a magnifications of ×10 to ×15 (Figure 1A). The AA
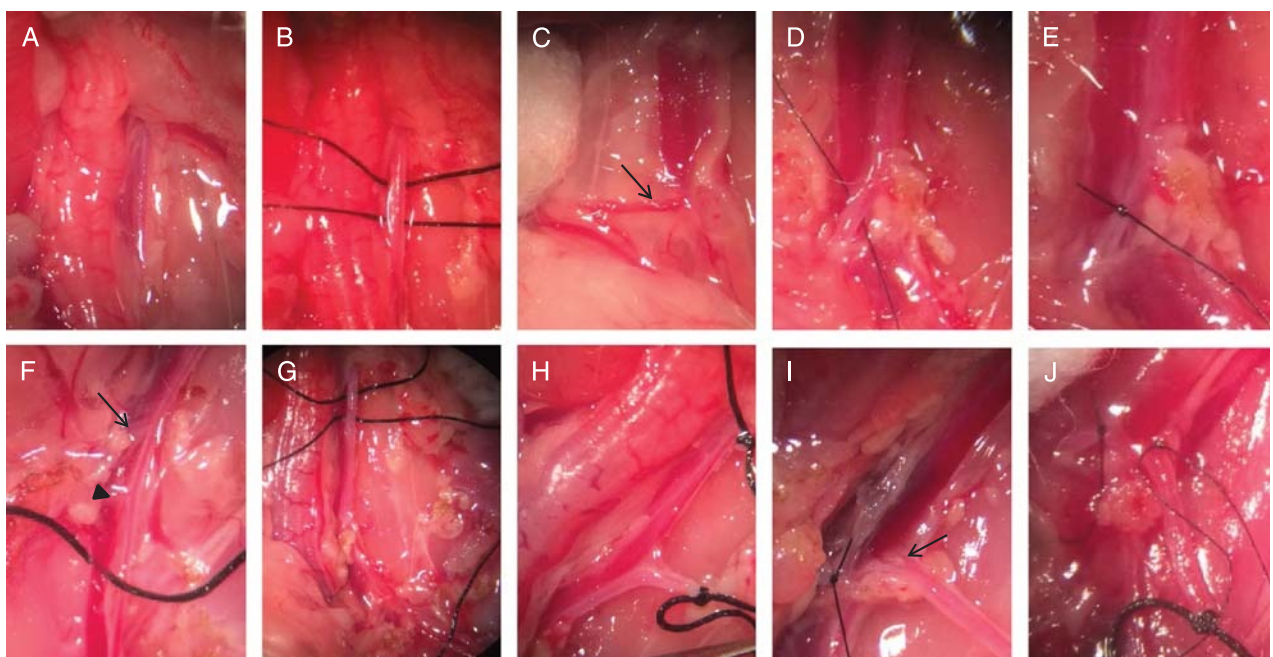
FIGURE 1. Representative photomicrograph for a donor's surgery via a dissecting scope (magnification, ×10-15) shows the AA (A) and anchored with two 6-0 silk sutures (B). C, D, Inferior mesenteric artery was identified and cauterized. D, E, Right common iliac artery was anchored with 9-0 nylon suture and ligated. F, Left femoral vein was anchored with 6-0 black silk, and left internal iliac (arrow) and medial femoral (arrowhead) arteries were identified. G, A whole arterial segment of the donor. H, The AA was dissected with microscissors. I, J, Middle caudal artery (arrow) was identified, and ligated with 9-0 nylon suture tie.

was anchored with two 6-0 black silks at the level of the inferior pole of the left kidney (Figure 1B). The inferior mesenteric artery was identified and cauterized (Figures 1C, D), and then the right common iliac artery was suture ligated with 9-0 nylon tie (Figures 1D, E). Another 2-cm longitudinal incision was made on the thigh above the femoral artery in the left inguinal region. The subcutaneous fat pad in the thigh was then visible, and it was necessary to retract the fat pad to isolate the left superficial femoral artery and vein without injury. Branches of the superficial artery and vein were cauterized as needed. The superficial femoral artery and vein were encircled and the vein was anchored with 6-0 silk suture near the inguinal ligament (Figure 1F). The segment of artery between the AA and the femoral artery was identified (Figure 1G), and the AA was dissected from the inferior vena cava (Figure 1H) with microscissors. The middle caudal artery was identified near the iliac bifurcation, and was ligated with a 9-0 nylon suture tie (Figures 1I, J). The femoral vein was cut at the level of the inguinal ligament with microscissors, and then the internal iliac artery and medial femoral artery were cauterized (Figure 2A). A 2- and 3-mm-long microtube cuff was prepared for the femoral vein and the AA, respectively, to interface with the microtubes (MicroLumen, Oldsmar, FL) made of polyamide (inner diameter, 0.4 mm; outer diameter, 0.45 mm; wall thickness, 0.023 mm) (Figure 2B). After applying a proximal vascular clamp, the distal cut end of the femoral vein was pulled through the 2-mm microtube cuff and everted to expose the endothelial surface. The vein was secured to the cuff with two 11-0 nylon ties (Figure 2C). The graft was flushed with 500 μL of heparin (Medefil, Inc., Glendale Heights, IL) (50 IU/mL) through the AA stump using a 30-gauge needle for anti-coagulation (Figure 2D).

Next, the 3-mm cuff was mounted onto the donor's AA in the same fashion as the femoral vein (Figure 2E-G). All muscle groups were sharply divided using cautery, and osteotomy was performed with a bone cutter at the level of the distal third of the femur. The harvested graft was stored in 50 IU/mL of heparin solution in ice until transplantation (Figure 2H).

Recipient Procedure

Before the surgery 0.5 mL of normal saline (Baxter, Deerfield, IL) was injected into the recipient's back skin for hydration. After shaving and cleaning with alcohol, a 1.5-cm longitudinal incision was made in the left cervical region and the left submaxillary gland was removed using cautery. The distal left external jugular vein (EJV) and common carotid artery (CCA) were ligated with 6-0 black silk ties (Figure 3A). After applying a vascular clamp in the proximal part of the CCA, the CCA was cut in between the clamp and tie and the open end slid over the exposed donor cuff. This creates a functional end-to-end cuff anastomosis between the donor AA and the recipient CCA. The anastomosis was secured with a 9-0 nylon suture tie. This step is facilitated by a stabilizing clamp (Roboz, Gaitherburg, MD) (Figure 3B). Next, after applying a distal vascular clamp, a small venotomy was made with microscissors on the recipient's EJV. The exposed cuff of the donor femoral vein was inserted through the venotomy and secured with a 9-0 nylon suture tie (Figure 3C). Successful blood circulation was achieved by removing the vascular clamps (Figure 3D, E). The donor skin was sutured to the surrounding recipient skin with interrupted 6-0 black silk sutures (Figure 3F) and no additional heparin was used.
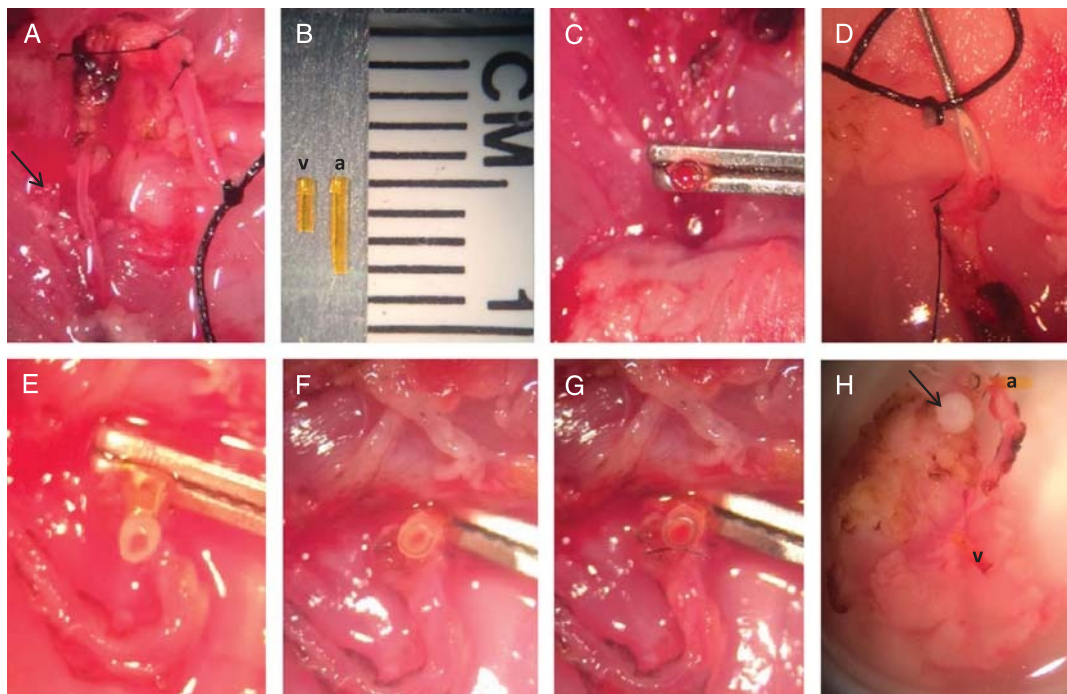
FIGURE 2. Surgical procedures of nonsuture cuff technique. A, The femoral vein (arrow) was cut near left inguinal ligament. B, Microtubes for femoral vein (v) and the AA (a). C, Femoral vein was mounted and secured with 11-0 nylon suture ties. D, Heparin solution was perfused through the AA stump. E, The AA was pulled through a microtube, and then (F) the AA was everted around the microtube. G, The AA was secured with 11–0 nylon suture ties. H, The completed donor graft including the AA (a), femoral vein (v), skin, fat, muscle, and femur (arrow).

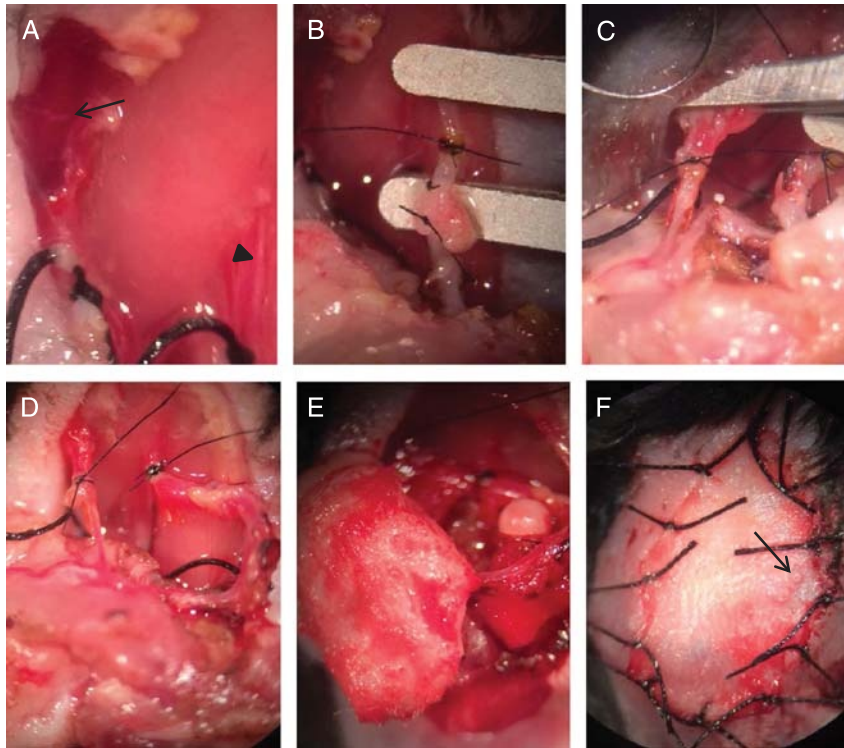**FIGURE 3.** Representative photomicrograph for the recipient procedure via a dissecting scope (magnification, ×15-20) shows left EJV (arrow) and CCA (arrowhead) (A). B, End-to-end anastomosis between the donor AA and the recipient CCA secured with a 9-0 nylon suture tie. C, A cuff of the donor femoral vein was inserted to the recipient's EJV after applying a vascular clamp, and secured with a 9-0 nylon suture tie. D, Revascularization after removing clamps. E, The viable transplanted graft. F, Skin repair with interrupted 6-0 black silk sutures, and a mouse nipple (arrow) was recognized.

Tacrolimus

In immunosuppressed mice, tacrolimus (Sigma-Aldrich, St. Louis, MO) in doses of 3 mg/kg were injected subcutaneously with a microsyringe (Hamilton, Reno, NV) daily. Tacrolimus was dissolved with 80% of 200 proof ethanol (Pharmaco-AAPER, Brookfield, CT) and 20% of castor oil (Sigma-Aldrich).

Assessment of Rejection Grade

After standard euthanasia, grafted tissue was harvested and fixed in optimal cutting temperature compound (Sakura Fineteck USA Inc., Torrance, CA). Eight days after VCA, 9-μm-thick graft sections were obtained using a cryotome (Thermo Fisher Scientific, Waltham, MA). Each section underwent hematoxylin-eosin (H&E) (Sigma-Aldrich) staining and examination for rejection grade by microscopy (Olympus, Hamburg, Germany). Image capture was performed with a SPOT RT color camera (Diagnostic instruments Inc, Sterling Heights, MI).

Device Setup and Data Processing

A portable class 1 LSI (MoorFLPI; Moor Instruments, Axminster, UK) with an integrated charge-coupled device camera allowed for dynamic acquisition of 2D, color-coded maps of perfusion. The imager was fixed to a clamped joint and attached to an operation desk. For purposes of data collection, the imager was connected to a computer (Dell Computer Cooperation, Round Rock, TX) through universal serial bus and FireWire interfaces. The LSI was positioned 30 cm above and perpendicular to the area of interest. Direct illumination of the field by light sources other than the laser light was avoided. For measurement of perfusion, the temporal filter was set to 25 frames per image and the graft perfusion was recorded with data acquisition software (MoorFLPI Measurement Software, Version 3.0; Moor Instruments). Transplanted tissue graft-Flux was calculated via review software (MoorFLPI Review Software) on the basis of recorded LSI. A user-defined region of interest was placed within the imaging field and the mean transplanted graft within the region of interest was calculated.

Statistical Analysis

Comparison between groups was performed using Student t test, and statistical significance was accepted with P less than 0.05.

RESULTS

Procedural Proficiency and Complications

To estimate the learning curve associated with this technique, a single investigator (M.K.) performed approximately 40 VCAs over the course of 3 months to establish the techniques before reporting the currently presented transplantation data. After the initial learning period, 30 VCAs were performed with a donor surgery time of 52 ± 10 minutes and a recipient surgery time of 45 ± 8 minutes. Successful graft circulation was obtained in 27 of 30 cases (90%). No mortality occurred directly related to the procedure. Most surgical complications occurred in 48 hours, such as 2 artery occlusions, 1 venous occlusion, 1 cerebral stroke, and minor

postoperative bleeding. Minor postoperative bleeding typically stopped spontaneously within 2 hours of procedure completion. One of the artery occlusions was detected 3 days after VCA. Despite study groups receiving immunosuppression, clinically evident infectious complications were not observed in this study.

Composite Tissue Allograft Longevity

Without any immunosuppressive agent, the average graft survival of a major histocompatibility complex (MHC)-mismatched recipient was 7 ± 1 day. All allogeneic recipients that did not receive tacrolimus developed explicit signs of acute rejection including dark discoloration and contracture of the skin that rapidly progressed to skin necrosis. The delineation between epidermis and dermis was lost microscopically, and lymphocyte infiltration in the skin and muscle was more extensive compared with well-tolerated grafts. In addition, vacuolization of muscle fiber was detected (Figures 4A-C). Tacrolimus (Sigma-Aldrich) given at 3 mg/kg per day significantly prolonged graft survival out to 30 days with rejection noted 7 to 14 days after cessation of immunosuppression (Figures 4D-F). Histological findings of tacrolimus-treated mice reflected similar patterns to syngeneic VCA transplanted mice with minimal lymphocyte

infiltration. All syngeneic grafts survived long term (>60 days) without signs of acute or chronic rejection (Figure 4G-I).

Graft Patency of the VCA Graft

LSI device setup for imaging was simple and straightforward (Figure 5A). Images of a donor skin showed a well-perfused groin region (Figure 5B). Recipients undergoing successful VCA revascularization demonstrated blood perfusion in the transplanted AA, femoral artery, and skin (Figure 5C) which could be visualized and measured. The skin perfusion after successful completion of VCA transplantation was similar to perfusion before VCA except for the interface of the graft and host skin (Figure 5D, E).

In one case of arterial occlusion, a signal could not be detected with intraoperative LSI in the graft, AA, and femoral vein (Figure 6A). The graft did not have any blood flow 1 day after VCA (Figure 6B) and the donor tissues underwent rapid necrosis from ischemia (Figure 6C). In another case of a potential vascular complication, blood flow was detected in the AA and the graft, but not the femoral vein which was indicative of venous obstruction (Figure 6D). This real-time finding allowed for a revision of the venous anastomosis (Figure 6E). At the end of the recipient surgery, a normal level of blood flow was noted by LSI in the skin of the VCA (Figure 6F). In recipients undergoing VCA revascularization,
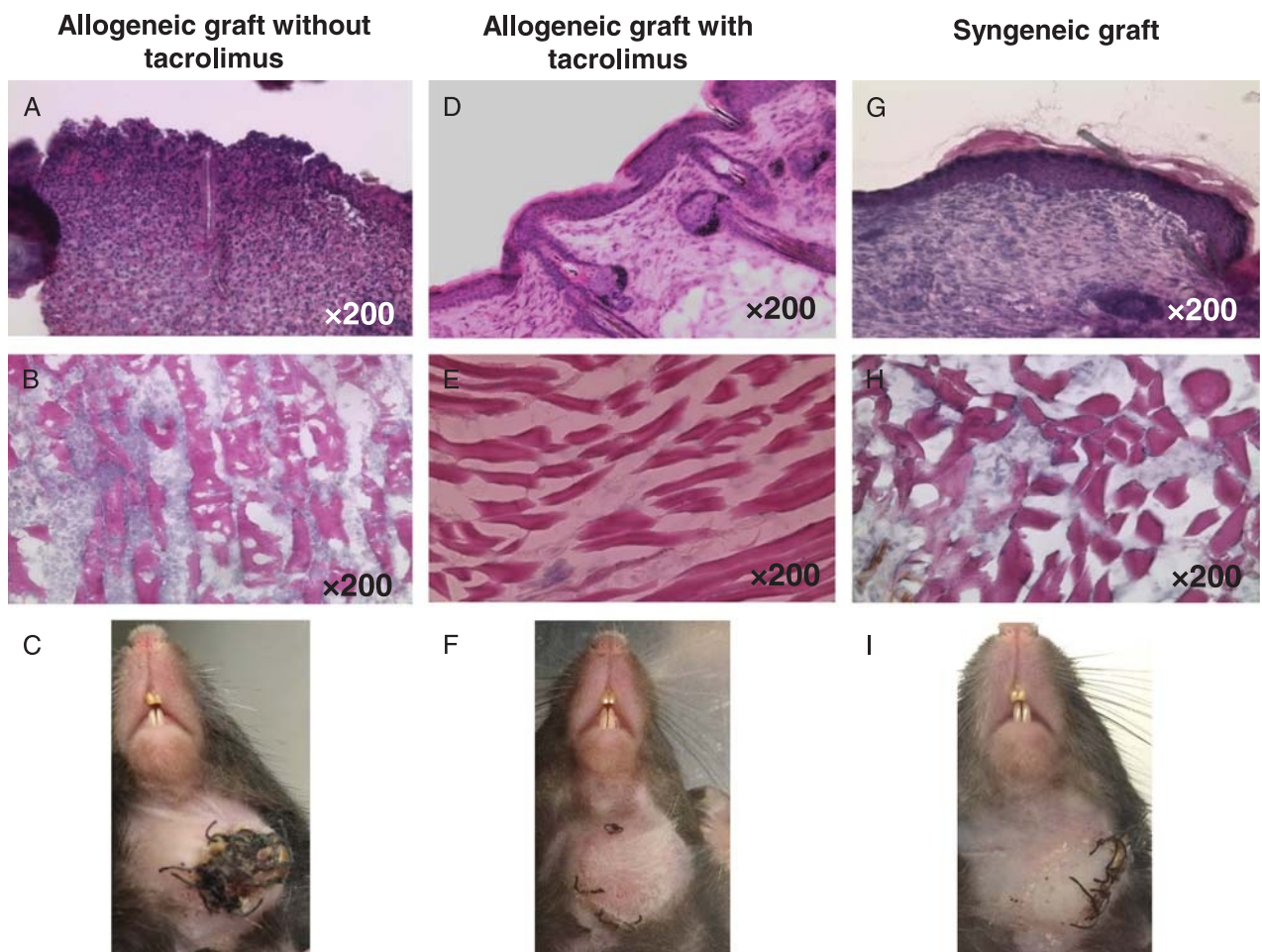

| Allogeneic graft without tacrolimus | Allogeneic graft with tacrolimus | Syngeneic graft |

FIGURE 4. H&E characteristics and gross findings of grafts 8 days after VCA. A-C, Severe allogeneic graft rejection was identified with aggressive lymphocytes infiltration, vacuolization of muscle fiber, and skin color change. D-F, Well-tolerated allogeneic graft with tacrolimus showed minimal lymphocytes infiltration in the graft and normal hair growing in the skin. G-I, Syngeneic graft showed intact skin and muscle.
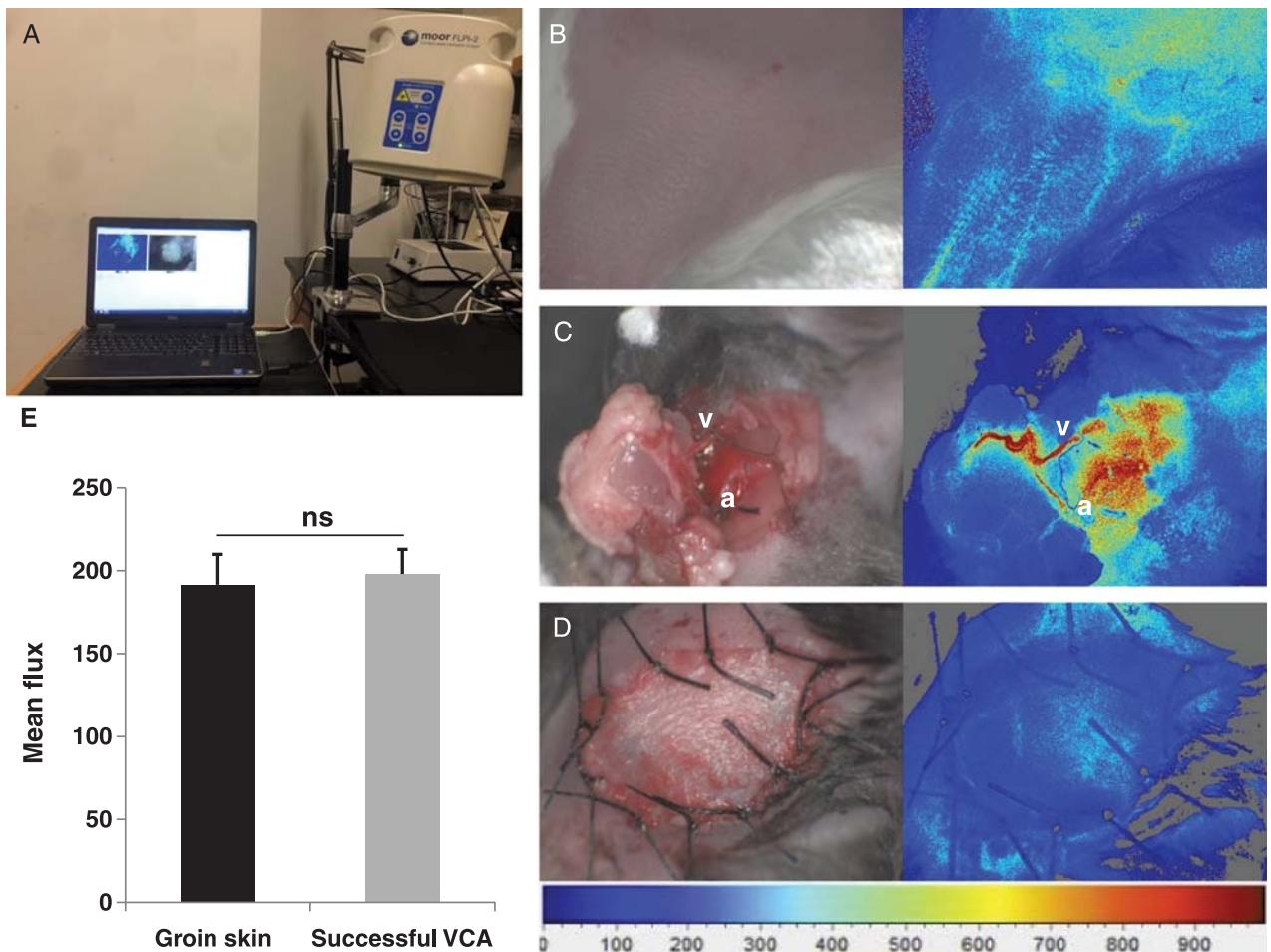
FIGURE 5. LSI device setup (A) Platform position and computer attachment. Gross speckle image and LSIs in left groin skin before VCA (B), in the AA (a) and the femoral vein (v) just after revascularization (C), and in the skin after the completion of VCA (D). E, Quantitative assessment of relative the graft blood flow before and after VCA (n = 4, P = 0.79). ns, not significant.

visual assessment by LSI of the AA and femoral vein corresponded to adequate graft perfusion and survival.

DISCUSSION

Patients who have VCA must endure a variety of serious lifelong toxicities such as infections, potential organ failure and cancer resulting from high doses of immunosuppressive drugs, while rejection rate of these types of composite grafts still remains disappointingly high.[16] For this reason, better immunosuppressive regimens are needed in VCA, and preclinical models are necessary to research this goal. Several techniques have been examined in mice and rats.[15,17,18] In this study, we described a novel method using the AA instead of the femoral artery for the arterial anastomosis, and introduced a new technique to detect intraoperative vascular complications.

The vessel anastomosis between the donor and recipient is the most technically difficult aspect of VCA. A nonsuture cuff technique for revascularization was reported in rats for VCA, and improved success rates of graft reperfusion were noted.[19] The technique was also adapted to a mouse model.[20,21] However, the mounting of a mouse femoral artery with a microtube is time-consuming due to the diminutive size of the femoral artery. Even though more collateral vessels

required ligation by using the AA, the donor surgery time was much shorter, 52 ± 10 minutes, than previously published methods using the femoral artery, 100 ± 12 minutes.[15] The use of electrocautery was the likely major time saver for the donor surgery. Because the AA was 2–3 times bigger than the femoral artery, mounting the artery around a microtube was simplified. In addition, the stump of the AA allowed for the flushing of heparin to minimize thrombosis. Also, as the AA has a larger diameter than the femoral artery, it would be anticipated that the transplanted graft would have a more consistent blood supply. Although the femoral vein is fragile, its size is similar to the AA, so mounting it onto the microtube was not difficult with delicate dissection. The overall success rate of VCA was 90% using our technique. The same diameter of microtube was fitted for the donor artery and vein, but the length for the AA was designed longer, making it easier to hold with a stabilizing clamp while performing the anastomosis. When considering an orthotopic VCA, these described techniques may not be applicable due to a long segment of the artery that may prevent orthotopic implantation. Success rates of an orthotopic model was only 62% by an experienced group,[15] so heterotopic VCA models may be better suited to investigate basic immunologic mechanisms of acute and chronic rejections and to test new immunosuppressive protocols.
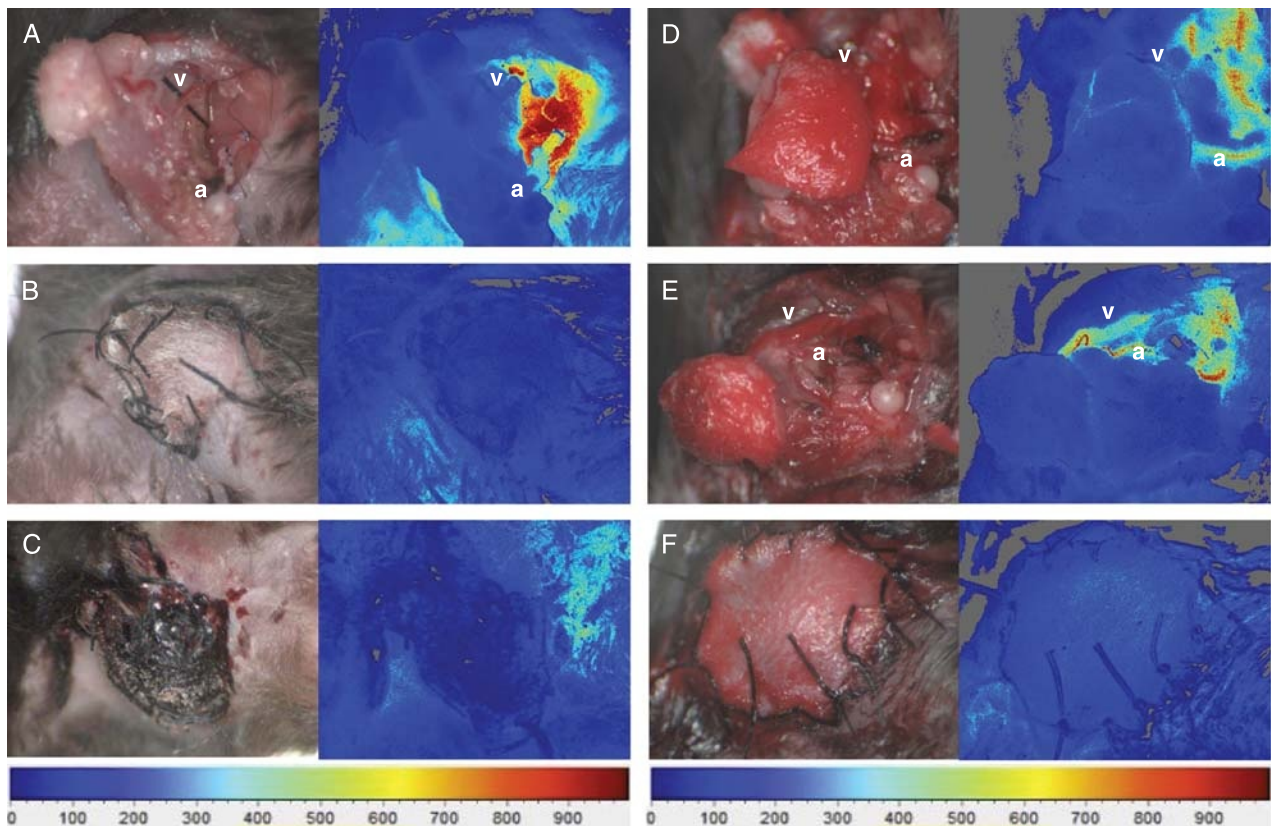
FIGURE 6. Intraoperative detection of vascular (a; AA, v; femoral vein) complications, gross speckle image and LSIs. A, No blood flow in "a" and "v" was detected in a case of arterial obstruction. B, No blood flow in the skin 1 day after arterial obstruction. C, The skin necrosis from ischemia after VCA. D, Blood flow was measured in "a" and the graft but "v" in a case of venous obstruction. E, Blood flow was detected in "v" after fixing venous anastomosis. F, 1 day after VCA.

Complication after VCA included 2 arterial occlusions, 1 venous occlusion, and 1 cerebral stroke. Most complications occurred within 48 hours. Arterial and venous occlusion showed different and distinct findings in the graft skin. The skin of the graft underwent rapid necrosis within 36 hours of arterial occlusion. During venous thrombosis, petechiae were detected in the skin first, followed by skin necrosis. Regarding cerebral stroke, the described model depends on an intact circle of Willis. If aberrant anatomy were present, a cerebrovascular event is possible and is manifested by a slow breathing pattern after occluding the left CCA during the procedure. After recovery, effected mice demonstrated motor signs of a left hemispheric stroke. The incidence of stroke was about 1 in 10 BALB/c mice and 1 in 30 C57BL/6 mice among 40 nonrecorded and 30 recorded VCAs for this study. Stroke could also result from blood clots in the graft, however, the use of heparin flushes should minimize this possibility. Furthermore, breathing pattern changes were detected after applying a vascular clamp on the CCA before revascularization, suggestive of ischemic stroke from occlusion, not embolism. Minor bleeding could be noted from the graft after revascularization indicating some degree of residual anticoagulation from heparin, but also adequate arterial blood flow to the graft. All episodes of minor bleeding resolved spontaneously and had no impact on graft survival. Without immunosuppression, allogeneic grafts showed severe rejection 7 ± 1 days after VCA. On the other hand, syngeneic grafts or allogeneic grafts treated with 3.0 mg/kg per day of tacrolimus did not show any signs of rejection for 30 days after VCA. The tacrolimus-treated allogeneic graft showed similar pathology findings compared to the syngeneic graft with a lesser amount of lymphocyte infiltration. In this study, we used syngeneic and allogeneic transplantation models to discern if complications were a result of anatomic variability or immunological responses to confirm the usefulness of the described modified technique.

The general application of LSI for noninvasive, real-time imaging of the transplanted graft including the AA, femoral vein, and skin was noteworthy. This relatively new technique was easy-to-use and acquired real-time blood flow images with high spatial resolution. Even though a high magnification was used for the surgery, visual confirmation of blood flow in the artery and vein is difficult to detect due to motion artifact from the beating heart, which may mask the graft blood flow particularly in cervical heterotopic transplantations. LSI assisted in the early identification of vascular complications, allowing for immediate reconstruction of the anastomosis. The main limitation of LSI was its lack of tissue penetration so that the main vessels could not be visualized after skin closure. However, detection of flow in superficial vessels of the graft suggests functional and adequate blood circulation.

Although outstanding progress has been made in VCA, the rejection rate of these composite grafts remains high due to MHC-mismatched cadaver-derived allografts. As a result, high-dose immunosuppressive medications are required, but with significant toxicity to the patient. The medications that are needed to maintain graft survival increase the recipient's

risk for opportunistic infections, hyperglycemia, hepatotoxicity, nephrotoxicity, reproductive toxicity, and cancer development.[12] Therefore, a major medical need is to discover new ways to both increase VCA graft tolerance and reduce the side effects of conventional immunosuppressive medications. In addition, early diagnosis of acute rejection is crucial for applying early medical or surgical interventions to save a transplanted graft after VCA. A punch skin biopsy in the graft is currently the primary method to monitor for signs of rejection; however, this technique is invasive and difficult to predict the stage and prognosis of rejection.[22] To overcome these obstacles, a feasible and reliable preclinical model is necessary for immunologic studies and the detection of early graft rejection. We believe that this modified cuff technique will allow researchers to have more consistent data after VCA to clarify effects of new immunosuppressive regimens, and LSI could be a noninvasive tool to detect early subclinical rejections before severe clinical rejections.

REFERENCES

1. Petit F, Minns AB, Dubernard JM, et al. Composite tissue allotransplantation and reconstructive surgery: first clinical applications. *Ann Surg*. 2003; 237:19–25.
2. Siemionow M, Kulahci Y. Facial transplantation. *Semin Plast Surg*. 2007; 21:259–268.
3. Devauchelle B, Badet L, Lengele B, et al. First human face allograft: early report. *Lancet*. 2006;368:203–209.
4. Dubernard JM, Owen ER, Lanzetta M, et al. What is happening with hand transplants. *Lancet*. 2001;357:1711–1712.
5. Gilbert R. Transplant is successful with a cadaver forearm. *Med Trib Med News*. 1964:20–23.
6. Morelon E, Petruzzo P. Vascularized composite allotransplantation still remains an emerging field after 17 years. *Curr Opin Organ Transplant*. 2015; 20:593–595.
7. Ravindra KV, Xu H, Bozulic LD, et al. The need for inducing tolerance in vascularized composite allotransplantation. *Clin Dev Immunol*. 2012; 2012:438078.
8. Bozulic LD, Breidenbach WC, Ildstad ST. Past, present, and future prospects for inducing donor-specific transplantation tolerance for composite tissue allotransplantation. *Semin Plast Surg*. 2007;21: 213–225.
9. Klimczak A, Siemionow M. Immune responses in transplantation: application to composite tissue allograft. *Semin Plast Surg*. 2007;21: 226–233.
10. Eun SC. Composite tissue allotransplantation immunology. *Arch Plast Surg*. 2013;40:141–153.
11. Barker JH, Francois CG, Frank JM, et al. Composite tissue allotransplantation. *Transplantation*. 2002;73:832–835.
12. Petruzzo P, Lanzetta M, Dubernard JM, et al. The International Registry on Hand and Composite Tissue Transplantation. *Transplantation*. 2010;90: 1590–1594.
13. Cooley BC, Daley R. Free flap transplantation in mice. *Microsurgery*. 1998; 18:320–323.
14. Tung TH, Mohanakumar T, Mackinnon SE. Development of a mouse model for heterotopic limb and composite-tissue transplantation. *J Reconstr Microsurg*. 2001;17:267–273.
15. Sucher R, Lin CH, Zanoun R, et al. Mouse hind limb transplantation: a new composite tissue allotransplantation model using nonsuture supermicrosurgery. *Transplantation*. 2010;90:1374–1380.
16. Kueckelhaus M, Fischer S, Seyda M, et al. Vascularized composite allotransplantation: current standards and novel approaches to prevent acute rejection and chronic allograft deterioration. *Transpl Int*. 2016;29: 655–662.
17. Shapiro RI, Cerra FB. A model for reimplantation and transplantation of a complex organ: the rat hind limb. *J Surg Res*. 1978;24:501–506.
18. Hewitt CW, Black KS, Fraser LA, et al. Composite tissue (limb) allografts in rats. I. Dose-dependent increase in survival with cyclosporine. *Transplantation*. 1985;39:360–364.
19. Sucher R, Oberhuber R, Margreiter C, et al. Orthotopic hind-limb transplantation in rats. *J Vis Exp*. 2010.
20. Lin CH, Sucher R, Shih YC, et al. The neck as a preferred recipient site for vascularized composite allotransplantation in the mouse. *Plast Reconstr Surg*. 2014;133:133e–141e.
21. Furtmuller GJ, Oh B, Grahammer J, et al. Orthotopic hind limb transplantation in the mouse. *J Vis Exp*. 2016; 53483.
22. Hautz T, Zelger B, Brandacher G, et al. Histopathologic characterization of mild rejection (grade I) in skin biopsies of human hand allografts. *Transpl Int*. 2012;25:56–63.